AIP Advances

Gate controllability of $HfSiO_x$/AlGaN/GaN MOS high-electron-mobility transistor

Cite as: AIP Advances **10**, 065215 (2020); https://doi.org/10.1063/5.0012687
Submitted: 05 May 2020 . Accepted: 20 May 2020 . Published Online: 10 June 2020

Ryota Ochi, Erika Maeda, Toshihide Nabatame, Koji Shiozaki, Taketomo Sato, and Tamotsu Hashizume

Gate controllability of $HfSiO_x$/AlGaN/GaN MOS high-electron-mobility transistor

Cite as: AIP Advances 10, 065215 (2020); doi: 10.1063/5.0012687
Submitted: 5 May 2020 • Accepted: 20 May 2020 •
Published Online: 9 June 2020

Ryota Ochi,[1,a] Erika Maeda,[2,3] Toshihide Nabatame,[3] Koji Shiozaki,[4] Taketomo Sato,[1] and Tamotsu Hashizume[1,4,b]

AFFILIATIONS

[1] Research Center for Integrated Quantum Electronics (RCIQE), Hokkaido University, Sapporo 060-0813, Japan
[2] Shibaura Institute of Technology, Tokyo 135-8548, Japan
[3] International Center for Materials Nanoarchitectonics, National Institute for Materials Science (NIMS), Tsukuba, Ibaraki 305-0044, Japan
[4] Institute of Materials and Systems for Sustainability (IMaSS), Nagoya University, Nagoya 464-8601, Japan

[a] **Author to whom correspondence should be addressed:** ochi@rciqe.hokudai.ac.jp
[b] **E-mail:** hashi@rciqe.hokudai.ac.jp

ABSTRACT

Hafnium silicate ($HfSiO_x$) has been applied to AlGaN/GaN high-electron-mobility transistors (HEMTs) as a high κ gate dielectric. The $(HfO_2)/(SiO_2)$ laminate structure was deposited on the AlGaN surface by a plasma-enhanced atomic layer deposition, followed by a post-deposition annealing at 800 °C. The $HfSiO_x$-gate HEMT showed good transfer characteristics with a high transconductance expected from its κ value and a subthreshold swing of 71 mV/decade. For the metal–oxide-semiconductor (MOS) HEMT diode, we observed excellent capacitance–voltage (C–V) characteristics with negligible frequency dispersion. The detailed C–V analysis showed low state densities on the order of 10^{11} cm^{-2} eV^{-1} at the $HfSiO_x$/AlGaN interface. In addition, excellent operation stability of the MOS HEMT was observed at high temperatures up to 150 °C.

I. INTRODUCTION

GaN high-electron-mobility transistors (HEMTs) with high-frequency and high-power performances are very attractive for the fifth generation communication system, where the W- and E-band frequency operations with an output power of over 1 W will be required for power amplifier transistors.[1,2] At present, because of several advantages including simplicity, ease of fabrication, and high transconductance, the Schottky-gate (SG) structure is generally used in GaN HEMTs. In the high input RF power regime, however, the SG GaN HEMT may suffer from marked leakage currents due to input swings high enough to drive the gate to forward bias.[3] In addition, Gao *et al.*[4] recently reported that the forward gate-bias stress applied to the SG AlGaN/GaN HEMT significantly increased gate leakage currents. They concluded from photoemission microscope and transmission electron microscope observations that the chemical degradation of the Ni/AlGaN contact during the forward bias stress is responsible for such an increase in gate leakage currents.

To overcome these issues related to a SG structure, a metal–insulator (oxide)-semiconductor (MIS or MOS) structure is desirable for advanced GaN HEMTs. In fact, it was reported that the SiN-gate AlGaN/GaN HEMT effectively controlled the gate leakage current even under high input power conditions.[3] To develop stable and high-performance MIS GaN HEMTs, it is important to consider bandgap, permittivity, breakdown field, and chemical stability of insulators. In addition, high band offsets and low state density at insulator/GaN(AlGaN) interfaces are requisites for an excellent gate dielectric.[5,6] Recently, we have developed and investigated hafnium silicate ($HfSiO_x$) as a gate dielectric for GaN-based devices.[7,8] After a post-deposition annealing (PDA) at around 800 °C, we achieved chemically stable amorphous $HfSiO_x$ layers with a high κ,

a high breakdown field, and low state densities at the $HfSiO_x$/GaN interfaces. In addition, Miyazaki and Ohta[9] reported a relatively large bandgap (E_G = 6.5 eV) for $Hf_{0.66}Si_{0.34}O_x$. These physical properties are very attractive for robust and high-transconductance (g_m) operation of GaN-based HEMTs, which provides more degrees of freedom in the design of device structures. Li and co-workers[10,11] applied the $HfSiO_x$ gate to the AlGaN/GaN HEMT structure on Si. However, they reported polycrystalline $HfSiO_x$ without a composition ratio and high interface state densities in the MOS structure.[11] Accordingly, in this paper, we fabricated $HfSiO_x$/AlGaN/GaN HEMTs and carried out electrical characterization of the MOS HEMTs, focusing on gate controllability and MOS interface properties.

II. DEVICE STRUCTURE AND FABRICATION PROCESS

Figure 1 shows the MOS-HEMT structure. We used the $Al_{0.2}Ga_{0.8}N$/GaN heterostructure grown by metalorganic chemical vapor deposition on the free-standing GaN substrate, provided by SCIOCS.[12] The C-doped GaN acts as a high-resistivity layer. The density and the mobility of the two-dimensional electron gas (2DEG) were 6.5 × 10^{12} cm^{-2} and 1750 cm^2 V^{-1} s^{-1}, respectively. We fabricated two kinds of MOS HEMTs using Al_2O_3- and $HfSiO_x$-gate dielectrics, and compared their DC characteristics. The gate–drain and gate–source distances are 10 μm.

To prevent partial crystallization in the Al_2O_3 film at high temperatures, an ohmic electrode process was first carried out for the Al_2O_3-gate HEMT.[13] After the metallization annealing at 800 °C, the Al_2O_3 layer was deposited on the AlGaN surface at 300 °C by atomic layer deposition (ALD) using H_2O and trimethylaluminum as precursors. The specific permittivity and the thickness of Al_2O_3 were 8.5 nm and 29 nm, respectively. After the MOS-HEMT fabrication, we carried out post-metallization annealing (PMA) at 300 °C in N_2 for 10 min.[14–17] The PMA process is effective in controlling the state densities in the order of 10^{10} cm^{-2} eV^{-1} at the Al_2O_3/GaN interface.[15] We also observed that gate controllability and operation stability of MOS HEMTs were remarkably improved by PMA.[12,16,17]

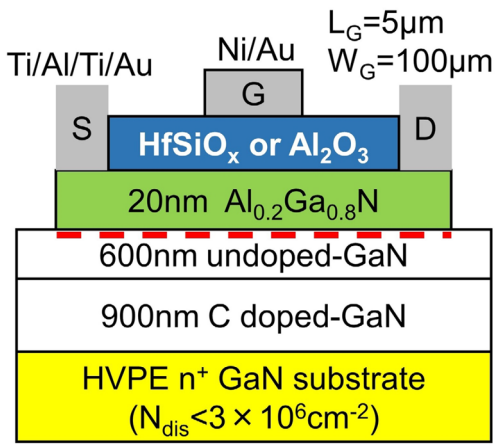

FIG. 1. Schematic illustration of the AlGaN/GaN MOS HEMT with $HfSiO_x$ or Al_2O_3 as a gate dielectric.

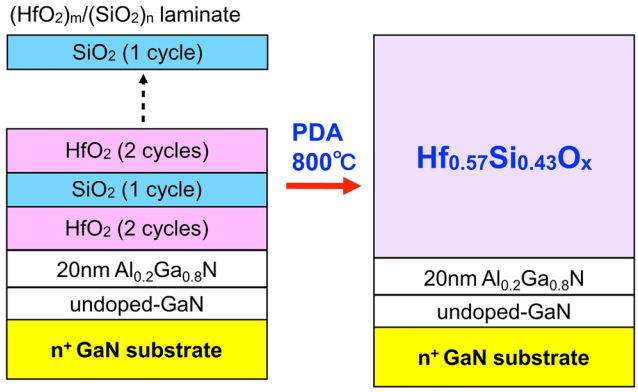

FIG. 2. Deposition procedure of the $(HfO_2)/(SiO_2)$ laminate and formation of the $HfSiO_x$ layer after PDA at 800 °C.

For the $HfSiO_x$-gate HEMT, the $(HfO_2)_m/(SiO_2)_n$ laminate structure, as shown in Fig. 2, was deposited on the AlGaN surface via plasma-enhanced ALD at 300 °C using tetrakis(dimethylamino) hafnium and tris(dimethylamino)silane precursors, along with a gaseous oxygen plasma.[7] The subscript indexes (m and n) indicate the numbers of ALD cycles for HfO_2 and SiO_2, respectively. In this study, we used m = 2 and n = 1, resulting in the $Hf_{0.57}Si_{0.43}O_x$ film. To obtain chemically stable hafnium silicate with an amorphous

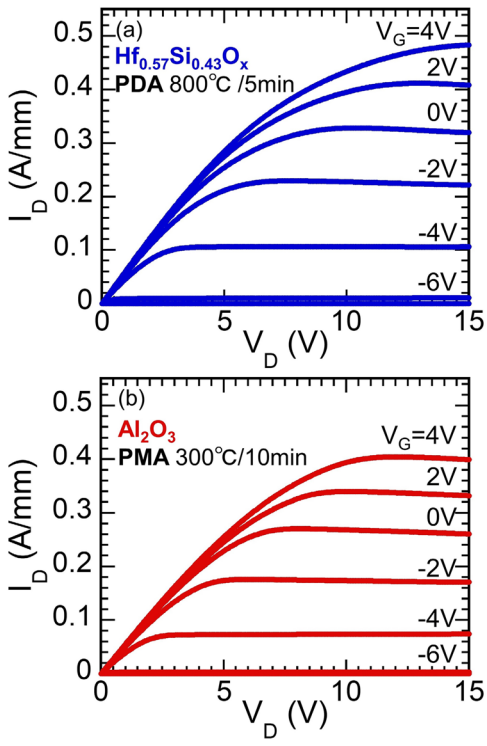

FIG. 3. Typical drain I–V characteristics of MOS HEMTs with (a) $HfSiO_x$ and (b) Al_2O_3 gates.

structure, we carried out PDA at 800 °C for 5 min in N_2.[7] The specific permittivity and the thickness of $Hf_{0.57}Si_{0.43}O_x$ were 13 nm and 32 nm, respectively.

III. RESULTS AND DISCUSSION

Typical drain I–V characteristics of MOS HEMTs with $Hf_{0.57}Si_{0.43}O_x$ and Al_2O_3 gates are shown in Fig. 3. Both devices exhibited good I–V behavior. The transfer characteristics of MOS HEMTs are shown in Fig. 4(a). For comparison, their transfer curves are plotted as functions of gate overdrive voltage in excess of threshold voltage ($V_G - V_{TH}$), where V_{TH} was defined as V_G giving an I_D of 1 μA/mm. It was found that the $Hf_{0.57}Si_{0.43}O_x$-gate HEMT showed a higher maximum g_m, as anticipated due to the higher κ of $Hf_{0.57}Si_{0.43}O_x$ than that of Al_2O_3. From the total capacitance of the insulator and AlGaN barrier in series, an 18% increase in g_m is expected for the $Hf_{0.57}Si_{0.43}O_x$-gate HEMT. The result in Fig. 3(a) is in good agreement with the simple estimation.

Figure 4(b) shows the semi-log scale I_D–V_G characteristics. The $Hf_{0.57}Si_{0.43}O_x$-gate HEMT showed a deeper V_{TH} than the Al_2O_3-gate HEMT. In the case of the $HfSiO_x$/GaN diode structure,[7] the negative shift of the flatband voltage was observed in the C–V curve, probably owing to the existence of positive fixed charges in the $HfSiO_x$ film or near the $HfSiO_x$/GaN interface. It is likely that a similar effect caused the deeper V_{TH} for the $HfSiO_x$-gate HEMT. For both devices, we observed low values of subthreshold swing (SS),[18] indicating excellent gate controllability of the MOS HEMTs. In addition, both devices exhibited very low leakage currents, corresponding to "gate" leakage currents. This means extremely low "drain" leakage currents below the detection limit as a result of the high-quality HEMT structure are grown on the GaN substrate with a low dislocation density that prevents bulk leakage conduction.[12] In fact, we observed a high on/off current ratio of around 5×10^9.

To investigate interface state properties of $HfSiO_x$/AlGaN and Al_2O_3/AlGaN structures, we carried out capacitance–voltage (C–V) characterization on MOS diodes fabricated on the same AlGaN/GaN heterostructures. A Ni circular gate with a diameter of 100 μm was prepared on oxide surfaces of the MOS diodes. C–V curves measured at frequencies of 1 kHz–1 MHz are shown in Fig. 5. Both diodes showed the two-step feature typically observed in C–V curves of HEMT-MOS structures,[19,20] indicating good gate control of the AlGaN surface potential. In particular, an extremely small frequency dispersion was observed in C–V curves for the $HfSiO_x$-HEMT structure, as evident in the enlarged view shown as the inset of Fig. 5(a). To evaluate the effects of interface states on the C–V characteristics quantitatively, we carried out a one-dimensional simulation with self-consistent Poisson–Schrödinger calculations[16,21] for MOS HEMTs. The detailed simulation procedure is described in Ref. 21.

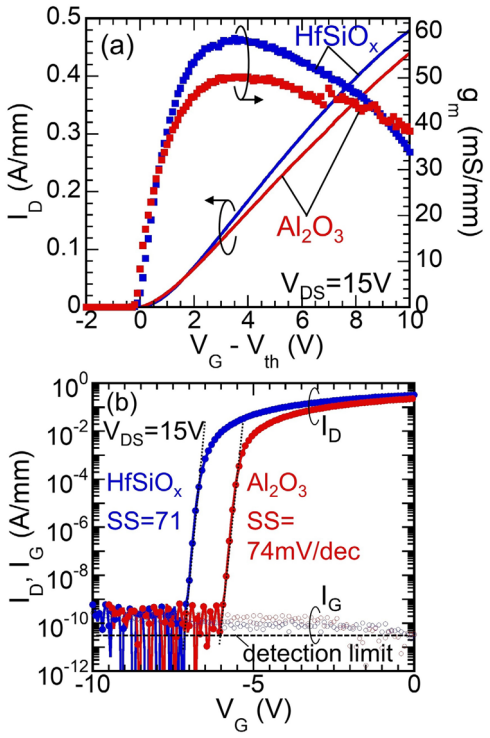

FIG. 4. (a) Transfer characteristics of MOS HEMTs with $HfSiO_x$ and Al_2O_3 gates. For comparison, transfer curves are plotted as functions of gate overdrive voltage in excess of threshold voltage (V_G–V_{TH}). (b) Semi-log scale I_D–V_G and I_G–V_G characteristics of MOS HEMTs.

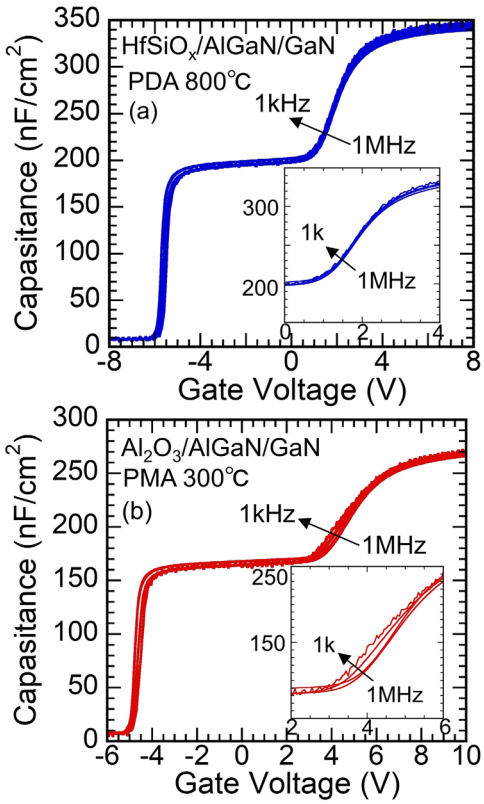

FIG. 5. C–V curves measured at frequencies of 1 kHz–1 MHz for MOS diodes with (a) $HfSiO_x$ and (b) Al_2O_3 gates fabricated on AlGaN/GaN heterostructures. The insets show enlarged C–V curves.

In the calculation, we assumed interface state density (D_{it}) distributions consisting of acceptor- and donor-like states separated by the charge neutrality level. Physical parameters reported in Ref. 16 were used in the calculation. For the $HfSiO_x$-HEMT sample, in addition, we used 13.0 eV, 6.5 eV, and 1.1 eV as κ, E_G, and the conduction band offset of the $HfSiO_x$/AlGaN interface,[9,22] respectively.

An example of the fitting result for the $HfSiO_x$/AlGaN sample is shown in Fig. 6(a). The calculation well reproduced the experimental capacitance within the entire range of applied gate bias. From the best fit of the calculated and measured C–V curves, D_{it} distributions were estimated for both MOS-HEMT diodes. Figure 6(b) shows D_{it} distributions at Al_2O_3/AlGaN and $HfSiO_x$/AlGaN interfaces. In this case, we estimated electron emission time constants (τ_e) from interface states to the conduction band at RT, using Shockley–Read–Hall (SRH) statistics.[16,21] The calculation showed that electrons once captured at interface states at energies below E_C − 0.8 eV remain trapped, owing to large τ_e at RT, even when large negative bias is applied to the gate electrode. Then, we ruled out the possibility of such "frozen states" for the calculation fitting of experimental C–V results, as shown in Fig. 6(b).

The $HfSiO_x$/AlGaN interface showed low interface state densities in the order of 10^{11} cm^{-2} eV^{-1} almost throughout the given energy range. The minimum density is $2 \times 10^{11} cm^{-2}$ eV^{-1}. This is consistent with extremely small frequency dispersion in C–V curves, as shown in Fig. 5(a). Hori *et al.*[23] reported that interface states at energies close to E_C can respond to the ac measurement signal, resulting in a parasitic capacitance in addition to the true MOS capacitance. The lower ac frequency corresponds to the wider energy range of states, contributing to the larger parasitic capacitance. Moreover, the higher the density of interface states, the higher the degree of frequency dispersion in C–V curves.[23] In the case of the $HfSiO_x$-HEMT diode, therefore, the negligibly small frequency dispersion shown in Fig. 5(a) also reflected low state densities at the $HfSiO_x$/AlGaN interface. It is likely that the PDA process at 800 °C is effective in recovering surface defects such as vacancies and in terminating dangling bonds with O atoms at the AlGaN surface.[15,24]

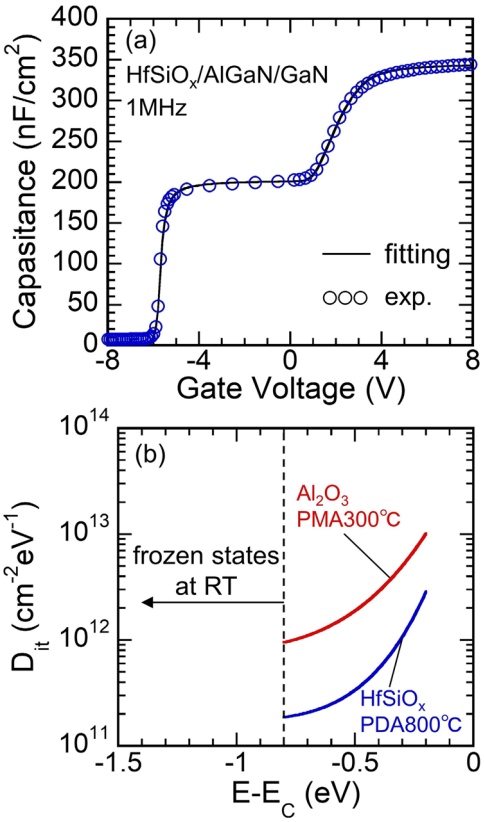

FIG. 6. (a) The best fitting result to experimental C–V plots (1 MHz). (b) Interface state density (D_{it}) distributions at $HfSiO_x$/AlGaN and Al_2O_3/AlGaN interfaces extracted from the fitting result.

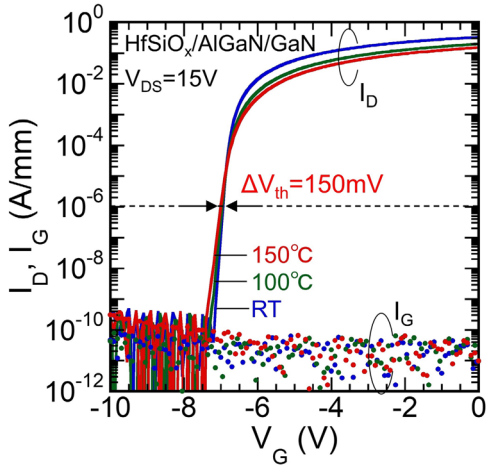

FIG. 7. Temperature-dependent transfer characteristics of the $HfSiO_x$-gate HEMT. V_{TH} was defined as V_G giving an I_D of 1 μA/mm.

The temperature dependence of transfer characteristics under V_{DS} = 15 V is shown in Fig. 7. Although on-state drain current decreases with increasing temperature, mainly owing to the decrease in electron mobility,[25,26] we observed smooth and steep subthreshold curves at high temperatures for the $HfSiO_x$-gate MOS HEMT. Even at 150 °C, the MOS HEMT showed stable operation with the V_{TH} drift of only 150 mV from its RT value, indicating excellent gate controllability. In addition, the leakage current almost remained unchanged at high temperatures, well controlled by extremely low gate leakage currents close to the detection limit. This robust operation demonstrates the strong potential of the HfSiOx-gate AlGaN/GaN HEMT for high-power applications.

IV. CONCLUSION

In summary, we carried out comparative characterization of AlGaN/GaN MOS HEMTs with $HfSiO_x$- and Al_2O_3-gate dielectrics. For the $HfSiO_x$-gate HEMT, the $(HfO_2)/(SiO_2)$ laminate structure was deposited on the AlGaN surface by plasma-enhanced ALD, followed by PDA at 800 °C. This process realized an amorphous $Hf_{0.57}Si_{0.43}O_x$ layer with κ = 13. The $HfSiO_x$-gate HEMT showed good transfer characteristics with high g_m expected from its κ value

and a subthreshold swing of 71 mV/decade. From the corresponding MOS-HEMT diode, we observed excellent C–V characteristics with negligible frequency dispersion. The detailed C–V analysis using a self-consistent Poisson–Schrödinger calculation showed low state densities in the order of 10^{11} cm^{-2} eV^{-1} at the $HfSiO_x$/AlGaN interface. In addition, good operation stability of the $HfSiO_x$-gate HEMT was observed at high temperatures. Even at 150 °C, the HEMT showed a low leakage current of 1.0×10^{-10} A/mm and a V_{TH} drift of only 150 mV from its RT value. Thus, the present MOS technology using the $HfSiO_x$ gate leads to further progress of GaN MIS HEMTs as high-performance and reliable RF power transistors.

ACKNOWLEDGMENTS

This work was partially supported by JSPS KAKENHI Grant No. JP16H06421.

DATA AVAILABILITY

The data that support the findings of this study are available from the corresponding author upon reasonable request.

REFERENCES

[1]T. Ohki, A. Yamada, Y. Minoura, K. Makiyama, J. Kotani, S. Ozaki, M. Sato, N. Okamoto, K. Joshin, and N. Nakamura, IEEE Electron Device Lett. **40**, 287 (2019).
[2]K. Makiyama, S. Ozaki, T. Ohki, N. Okamoto, Y. Minoura, Y. Niida, Y. Kamada, K. Joshin, K. Watanabe, and Y. Miyamoto, in *2015 IEEE International Electronic Devices Meeting (IEDM), Washington, DC, 7-9 December 2015* (IEEE, 2015).
[3]M. Kanamura, T. Kikkawa, T. Iwai, K. Imanishi, T. Kubo, and K. Joshin, in *IEEE International Electronic Devices Meeting, 2005: IEDM Technical Digest, Washington, DC, 5 December 2005* (IEEE, 2005).
[4]Y. Gao, W. A. Sasangka, C. V. Thompson, and C. L. Gan, Microelectron. Rel. **100-101**, 113432 (2019).
[5]Z. Yatabe, J. T. Asubar, and T. Hashizume, J. Phys. D: Appl. Phys. **49**, 393001 (2016).
[6]T. Hashizume, K. Nishiguchi, S. Kaneki, J. Kuzmik, and Z. Yatabe, Mat. Sci. Semicond. Proc. **78**, 85 (2018).
[7]T. Nabatame, E. Maeda, M. Inoue, K. Yuge, M. Hirose, K. Shiozaki, N. Ikeda, T. Ohishi, and A. Ohi, Appl. Phys. Express **12**, 011009 (2019).
[8]E. Maeda, T. Nabatame, K. Yuge, M. Hirose, M. Inoue, A. Ohi, N. Ikeda, K. Shiozaki, and H. Kiyono, Microelectron. Eng. **216**, 111036 (2019).
[9]S. Miyazaki and A. Ohta, ECS Trans. **92**, 11 (2019).
[10]Q. Hu, S. Li, T. Li, X. Wang, X. Li, and Y. Wu, IEEE Electron Device Lett. **39**, 1377 (2018).
[11]S. Li, Q. Hu, X. Wang, T. Li, X. Li, and Y. Wu, IEEE Electron Device Lett. **40**, 295 (2019).
[12]Y. Ando, S. Kaneki, and T. Hashizume, Appl. Phys. Express **12**, 024002-1–024002-5 (2019).
[13]Y. Hori, C. Mizue, and T. Hashizume, Jpn. J. Appl. Phys., Part 1 **49**, 08001 (2010).
[14]S. Kaneki, J. Ohira, S. Toiya, Z. Yatabe, J. T. Asubar, and T. Hashizume, Appl. Phys. Lett. **109**, 162104 (2016).
[15]T. Hashizume, S. Kaneki, T. Oyobiki, Y. Ando, S. Sasaki, and K. Nishiguchi, Appl. Phys. Express **11**, 124102 (2018).
[16]K. Nishiguchi, S. Kaneki, S. Ozaki, and T. Hashizume, Jpn. J. Appl. Phys., Part 1 **56**, 101001 (2017).
[17]S. Ozaki, K. Makiyama, T. Ohki, N. Okamoto, Y. Kumazaki, J. Kotani, S. Kaneki, K. Nishiguchi, N. Nakamura, N. Hara, and T. Hashizume, Semicond. Sci. Technol. **35**, 035027 (2020).
[18]H. Tokuda, J. T. Asubar, and M. Kuzuhara, Jpn. J. Appl. Phys., Part 1 **56**, 104101 (2017).
[19]C. Mizue, Y. Hori, M. Miczek, and T. Hashizume, Jpn. J. Appl. Phys., Part 1 **50**, 021001 (2011).
[20]Z. Yatabe, Y. Hori, W.-C. Ma, J. T. Asubar, M. Akazawa, T. Sato, and T. Hashizume, Jpn. J. Appl. Phys., Part 1 **53**, 100213 (2014).
[21]M. Miczek, C. Mizue, T. Hashizume, and B. Adamowicz, J. Appl. Phys. **103**, 104510 (2008).
[22]X. Qin, L. Cheng, S. McDonnell, A. Azcatl, H. Zhu, J. Kim, and R. M. Wallace, J. Mater. Sci., Mater. Electron. **26**, 4638 (2015).
[23]Y. Hori, Z. Yatabe, and T. Hashizume, J. Appl. Phys. **114**, 244503 (2013).
[24]T. K. Zywietz, J. Neugebauer, and M. Scheffler, Appl. Phys. Lett. **74**, 1695 (1999).
[25]W. S. Tan, M. J. Uren, P. W. Fry, P. A. Houston, R. S. Balmer, and T. Martin, Solid State Electron. **50**, 511 (2006).
[26]Y.-H. Wang, Y. C. Liang, G. S. Samudra, T.-F. Chang, C.-F. Huang, L. Yuan, and G.-Q. Lo, Semicond. Sci. Technol. **28**, 125010 (2013).